Functional Materials Letters
Vol. 10, No. 5 (2017) 1750052 (5 pages)

DOI: 10.1142/S1793604717500527

World Scientific
www.worldscientific.com

In situ atomic force microscope observing the effect of vinylene carbonate on the formation of solid-electrolyte interphase layer during the initial cycle

Lingpiao Lin, Kai Yang, Haibiao Chen and Feng Pan*
School of Advanced Materials,
Peking University Shenzhen Graduate School
Shenzhen 518055, P. R. China
**panfeng@pkusz.edu.cn*

Received 9 June 2017; Accepted 3 July 2017; Published 26 July 2017

We used *in situ* atomic force microscope to observe the evolution of the solid-electrolyte interphase (SEI) layer on the graphite surface during the initial lithium intercalation process. We found that 1% vinylene carbonate (VC) in the electrolyte can promote the formation of an initial SEI at a higher potential by VC reduction. VC also restrained the reduction of ethylene carbonate (EC) and as a consequence, it can affect the morphology of the SEI formed.

Keywords: Solid electrolyte interphase; vinylene carbonate; *in situ* AFM.

Li-ion batteries (LIBs) are indispensable for today's electric transportation and portable electronic devices and recent developments are looking to further improve the energy density, power density, lifetime, and safety of LIBs. However, much of the chemistry and processes underlying the battery system still remain to be understood. During the initial charging and discharging process, a passivation layer formed at the solid–solution interface between the anode and the electrolyte and it is called a solid-electrolyte interphase (SEI) layer. An SEI layer has a high ionic conductivity and a low electronic conductivity, and imparts kinetic stability to the electrolyte against further reduction in successive cycles, thereby ensuring good cyclability of the electrode.[1] One approach to tune the properties of the electrolyte is to add various additives in the electrolyte for serving various purposes. Vinylene carbonate (VC) as a very important additive has been studied by many researchers.[2] 20% VC can promote the SEI formation on the surface of $Li_4Ti_5O_{12}$ (LTO) effectively.[3] Madec *et al.* found that adding 2% VC greatly improved the electrochemical performance and alleviated gas production in $LiNi_{1/3}Mn_{1/3}Co_{1/3}O_2$/graphite pouch cells.[4] Xiong *et al.* studied how temperature affected the performance of Li/graphite cells after adding VC, and found that coulombic efficiency increased by 0.0015 with VC.[5] Another study found that VC improved the cycling performance of the battery by minimizing the reaction of alkyl carbonate solvents and the resistance of the battery.[6] After adding VC in $LiClO_4$ electrolyte, the thickness of the precipitate layers was estimated to be less than half of that without VC.[7]

Previous studies on the effect of the additives on the SEI layer mostly relied on *ex situ* characterization techniques such as GC-MS, X-ray photoelectron spectroscopy (XPS), and SEM. Very few studies focused on how the additive influences the formation of an SEI film, especially during the initial cycle. *In situ* atomic force microscope (AFM) as a direct way has been used in researching the change of the morphology of the electrode surface in LIBs in recent years,[8–11] especially for investigating the evolution of the SEI layer on the graphite anode.[12,13] It can be used in combination with electrochemical control and well simulates a real device with minimal interference.

Effect of low concentration VC on the formation of the SEI layer on graphite in $LiPF_6$ EC/DMC electrolyte has not been investigated previously. In this work, we observed the change in the morphology of the SEI layer on graphite surface after 1% VC was added to the electrolyte by *in situ* AFM and found great differences between a regular electrolyte and a 1% VC-added electrolyte. Results of *in situ* AFM can be used to evaluate how a low concentration VC can impact the SEI layer and can be used to predict the performance of an LIB. XPS was employed to verify the effect of VC on the composition of the SEI layer.

The set-up of *in situ* AFM measurement is schematically shown in Fig. 1. The AFM cell was composed of a highly oriented pyrolytic graphite (HOPG, $12 \times 12 \times 2\,mm^3$, ZYB

*Corresponding author.

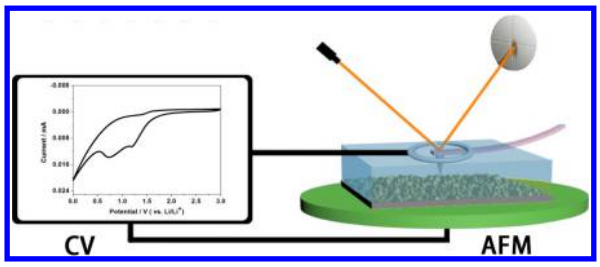

Fig. 1. Schematic of *in situ* AFM cell configuration for measuring CV and surface morphology simultaneously. The cell was connected to an electrochemical workstation and an AFM imaging control system.

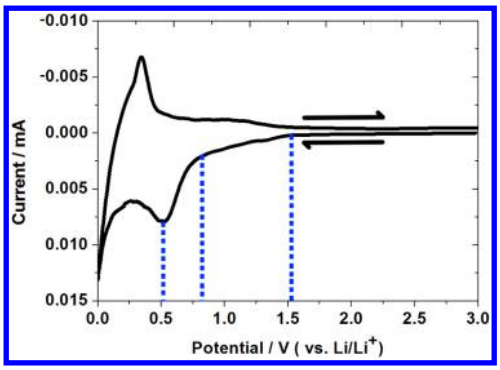

(a)

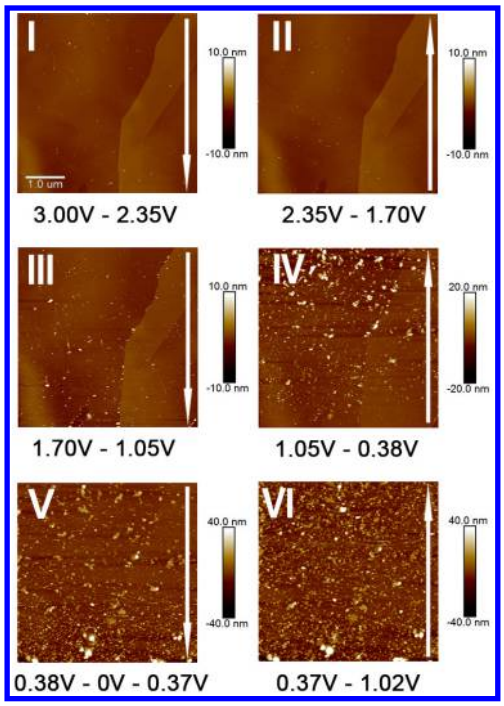

(b)

Fig. 2. (a) CV curves of the freshly cleaved HOPG electrode in 1.0 M $LiPF_6$/EC/DMC at scan rate of 2 mV/s. Arrows indicate that the scanning direction is 3.00–0–3.00 V. (b) *in situ* AFM imaging of SEI formation on HOPG with the CV scan from 3.00–0–3.00 V. The white arrows indicate the scanning directions.

Grade, Bruker Corporation) substrate cleaved with adhesive tape to expose a fresh surface as the working electrode (WE, Fig. S2), a Li wire as the counter and reference electrodes (CE and RE), and a 1.0 M $LiPF_6$ ethylene carbonate/dimethyl carbonate solution (EC/DMC, volume ratio of 1:1) as the regular electrolyte or with 1 wt.% VC was injected into the cell. The HOPG substrate was mounted at the bottom of the AFM fluid cell (MMTMEC type) and Li wire was placed inside the round cell groove (Fig. S1). *In situ* AFM experiment was carried out with an AFM system (Bruker Multimode 8 with a Nanoscope *V* controller) in an argon-filled glovebox (MIKOUNA, $H_2O \leq 0.1$ ppm, $O_2 \leq 0.1$ ppm) at room temperature. An external CH1030C electrochemical workstation was combined with the fluid cell to control the potential of the electrodes during AFM imaging. The SEI formation was studied by cyclic voltammetry (CV) at a scanning rate of 2 mV/s between 3.00 and 0 V. AFM topography was collected simultaneously in the Peakforce Tapping mode. In this mode, damage to the morphology can be effectively prevented when a fragile sample was tested.

Figure 2(a) shows the first CV curves of HOPG surface between the voltage range of 3.00–0 V in the regular 1.0 M $LiPF_6$/EC/DMC electrolyte. The current remained close to zero until the potential was lowered to 1.52 V and then slowly increased intensity after 1.52 V. At about 0.80 V, the magnitude of the current sharply increased and reached the peak value at 0.53 V. This sharply increased current intensity between 0.80 V and 0 V is corresponding to the reduction of EC with the lithium intercalation.[14] In the reverse scan, the anodic current gradually increased and reached the peak at around 0.30 V, corresponding to lithium deintercalation at the HOPG basal plane. Figure 2(b) shows the surface evolution of the HOPG electrode as observed by AFM during the CV scanning in Fig. 2(a). From 3.00 V to 1.70 V, no apparent substance formed on the HOPG electrode and the surface remained quite smooth (Figs. 2(b)(I) and 2(b)(II)). When the current started to increase in intensity, scattered fine particles began to appear uniformly on HOPG as shown in Fig. 2(b)(III), corresponding to the current change at 1.52 V. These particles are regarded as the reduction of oxygen dissolved in the solution as well as the contaminations.[15] When the potential continued to sweep to 0.70 V, a large number of bigger particles formed on the electrode surface as shown in Fig. 2(b)(IV) during scanning of CV as the current quickly increased intensity, corresponding to the cathodic peak at 0.52 V. This stage can be related to the initial growth of the SEI layer on the HOPG. However, the population density of the particles remained low until 0 V. When the potential continued to sweep from 0 V to 3.00 V, a higher population density of particles appeared and form a continuous layer together as seen in the lower region of the AFM image in Fig. 2(b)(V). There were no obvious changes in the

morphology when the potential swept from 0.37 V to 3.00 V in the anodic scanning (Figs. 2(b)(VI) and S3). It indicates that as the potential increased, the SEI layer stopped growing in the anodic scanning progress. Note that the images may shift slightly during AFM scanning, but the observation was not affected.

Figure 3 shows the first CV curves between the voltage range of 3.00–0 V in the 1.0 M $LiPF_6$/EC/DMC with 1% VC at a 2 mV/s scan rate. The cathodic current remained close to zero until 1.08 V and it began to increase the intensity. The intensity of the current sharply increased at about 1.52 V and

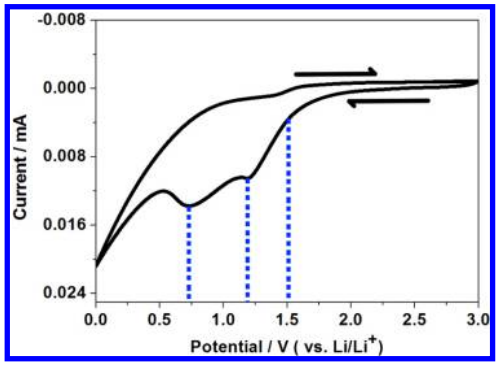

(a)

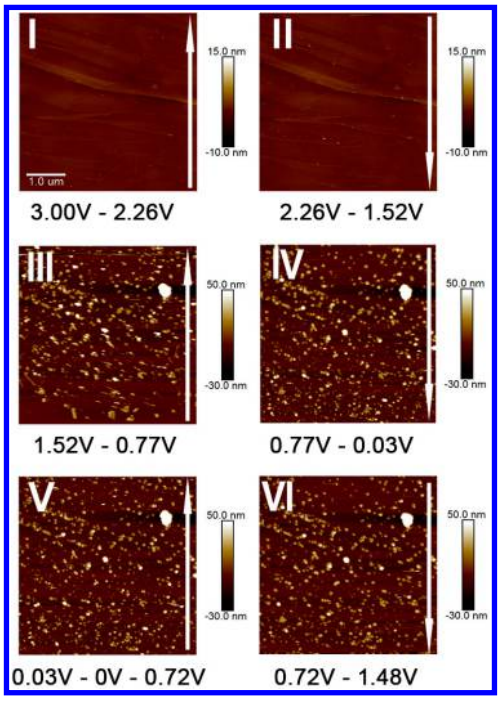

(b)

Fig. 3. (a) CV curves of the freshly cleaved HOPG electrode in 1.0 M $LiPF_6$/EC/DMC with 1% VC at a scan rate of 2 mV/s. Arrows indicate that the potential scanning direction is 3.00–0–3.00 V. (b) *in situ* AFM imaging of the SEI formation on HOPG with the CV scan from 3.00–0–3.00 V in 1.0 M $LiPF_6$/EC/DMC with 1% VC. The long white arrows indicate the scanning directions.

the first major cathodic peaks were observed at 1.20 V which may be contributed by the reduction of VC and it was higher than the reduction potential of EC. Similar to the regular electrolyte, the reduction of EC was taking place at about 0.74 V and lithium intercalation was taking place under 0.50 V. Interestingly, another feature different from the regular electrolyte is that during the anodic sweeping, there was almost no visible oxidation peak that could be related to the lithium deintercalation process.

Figure 3(b) shows the surface evolution of the HOPG electrode scanned at 2 mV/s between 3.00 V and 0 V during the first lithiation–delithiation cycle corresponding to the CV scanning shown in Fig. 3(a). Similar to the regular electrolyte, there is no precipitate formation until the current started to increase the intensity. Figures 3(b)(I) and 3(b)(II) show a clean fresh surface of HOPG. As the potential scan continued, a large number of bulky particles appeared at around 1.50 V, just corresponding to the reduction current of VC started at 1.52 V (Fig. 3(b)(III)). Further scanning from 1.52 V to 0.03 V gradually produced more particles on the basal plane as shown in Figs. 3(b)(III) and 3(b)(IV). The particle-like morphology of the SEI formed in the VC-added electrolyte is similar to that formed in a regular electrolyte, however, the particles formed by the reduction of VC appeared to be larger than those formed in the regular electrolyte. Interestingly, we found that the reduction of EC can continue to form particles on the uncovered surface of HOPG. As Fig. 4(a) shows, the blue line A was drawn across the HOPG surface without touching any particles in an image scanning from 1.52 to 0.77 V, which was before the reduction of EC. The height profile along line A shows that the surface was relatively smooth. However, when the potential decreased to below 0.77 V, EC reduction occurred and along the same line (marked as green line B) the height profile shows much increased roughness (Fig. S5). In contrast, the particles formed by VC reduction remained almost no change between these two images. The observation indicates that EC reduction preferred to occur on the uncovered surface of HOPG rather than on top of the existing particles.

Compared to the morphology of the SEI formed in the regular electrolyte, VC may restrain the reduction of EC. As shown in Figs. 3(b)(V) and 3(b)(VI), the SEI formed on uncovered surface between the VC-generated particles is thin, but in the regular electrolyte, bigger particles are formed by EC reduction. We can propose a process of the surface evolution as shown in Fig. 4(c). First, VC reduction reaction occurred and formed many particles on the HOPG basal plane, and then EC reduction contributed to form a thin layer on the uncovered HOPG surface. Similar to the regular electrolyte, during the anodic scanning, the morphology remained unchanged which suggests that the growth of the SEI had stopped (Fig. S4).

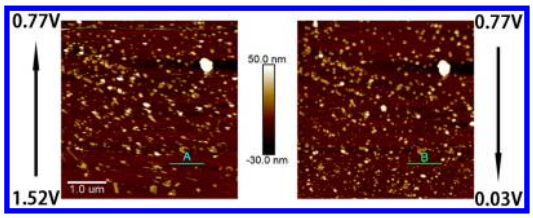

(a)

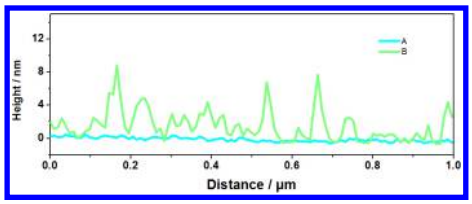

(b)

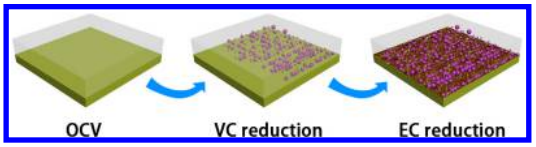

(c)

Fig. 4. (a) AFM imaging from 1.52 V to 0.77 V and from 0.77 V to 0.03 V in 1.0 M $LiPF_6$/EC/DMC with 1% VC. (b) The height curve of surface morphology corresponding to the line A and B in the AFM image in Fig. 4(a). (c) The schematic of different surface evolution stage on HOPG electrode in 1.0 M $LiPF_6$/EC/DMC with 1% VC.

Since the AFM results provided little information on the chemistry, XPS was employed as a complementary tool to better understand the composition of the SEI formed with the VC additive. We analyzed the SEI in samples obtained at different stages of the first CV cycle using XPS under vacuum operation. As Fig. 5 shows, both samples show C–C signal at 284.8 eV and C–O at 286.8 eV which is attributed to carbon atoms of bare HOPG and the organic species of SEI.[12] However, signal of the C=O bonds from the VC sample is stronger than that from the regular electrolyte, indicating that the C=O bonds may mainly come from the product of VC reduction. The peak at 295.8 eV corresponds to the C–F bond from the product of $LiPF_6$ decomposition. In the O 1*s* core peak, oxygen atoms associated with $(ROCO_2Li)_2$ species represent the main contribution of the spectrum with an intense component located at 532 eV,[16] which come from the EC reduction reaction. However, the signal from the VC sample is weaker than that from the regular electrolyte, which can be a good evidence that VC may restrain further EC reduction. In the O1*s* spectra, obvious signal at 533.3 eV which corresponds to the C–O bond suggests that the product from VC reduction mainly contain C–O. O–H at 535.1 eV may come from trace water in the electrolyte. From the F 1*s* spectra, the weak signal of PF_6^- at 688 eV indicates the residual $LiPF_6$, and LiF at 685.2 eV should come from the product of $LiPF_6$ decomposition reaction. The results show that both kinds of SEI consist of $(ROCO_2Li)_2$ organic component and LiF inorganic component, but the product from VC mainly contain C=O and C–O bonds, and in the 1% VC-added electrolyte, the reduction of EC was restrained.

In summary, using *in situ* AFM technology, we observed morphological difference during the formation of the SEI layer between a regular electrolyte and a 1% VC-added electrolyte directly. The observation suggests that by adding VC, the SEI reduction reaction was promoted at a higher voltage compared to a regular electrolyte. When the potential of EC reduction was reached, EC can form a thin layer on the uncovered surface. In contrast, in the regular electrolyte, SEI is formed from large particles. Therefore, a low concentration of VC may have a suppressive effect on the reduction of EC reduction and produce a different type of SEI layer.

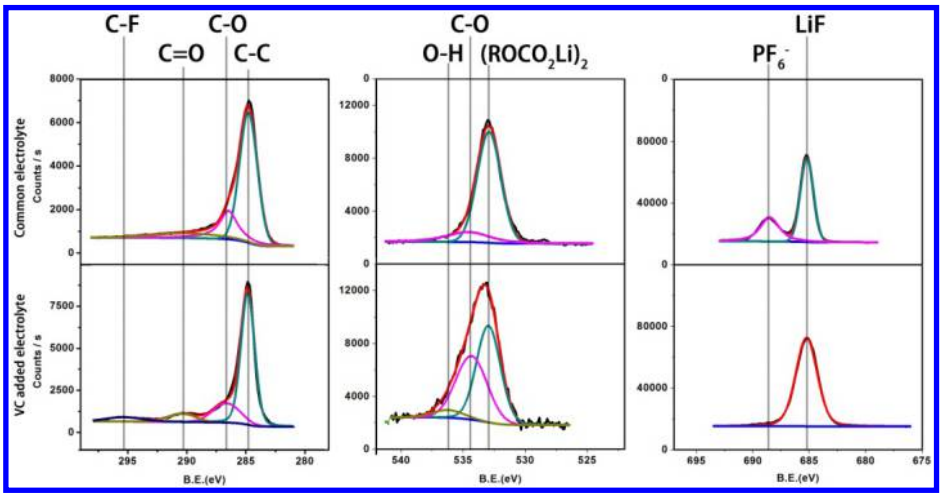

Fig. 5. C1*s*, O1*s*, F1*s* spectra of HOPG electrode from 1.0 M $LiPF_6$ EC/DMC electrolyte without and with 1% VC after first CV scanning.

Acknowledgments

This research was financially supported by the National Materials Genome Project (2016YFB0700600), the Guangdong Innovation Team Project (No. 2013N080), and the Shenzhen Science and Technology Research Grants (Nos. JCYJ20150626110958181, JCYJ20150518092933435).

References

1. K. Xu, *Chem. Rev.* **114**, 11503 (2014).
2. A. M. Haregewoin, A. S. Wotango and B.-J. Hwang, *Energy Environ. Sci.* **9**, 1955 (2016).
3. S. Wang, K. Yang, F. Gao, D. Wang and C. Shen, *RSC Adv.* **6**, 77105 (2016).
4. L. Madec, R. Petibon, K. Tasaki, J. Xia, J. P. Sun, I. G. Hill and J. R. Dahn, *Phys. Chem. Chem. Phys.* **17**, 27062 (2015).
5. D. Xiong, J. C. Burns, A. J. Smith, N. Sinha and J. R. Dahn, *J. Electrochem. Soc.* **158**, A1431 (2011).
6. T. Sasaki, T. Abe, Y. Iriyama, M. Inaba and Z. Ogumi, *J. Power Sources* **150**, 208 (2005).
7. D. Yasuhiro, O. Manabu. T. Shigetaka, N. Hiroe, Y. Toshiro, D. Takayuki, A. Takeshi and O. Zempachi, *J. Electrochem. Soc.* **159**, A1292 (2012).
8. J. Zhang, X. Yang, R. Wang, W. Dong, W. Lu, X. Wu, X. Wang, H. Li and L. Chen, *J. Phys. Chem. C* **118**, 20756 (2014).
9. A. Tokranov, B. W. Sheldon, C. Li, S. Minne and X. Xiao, *ACS Appl. Mater. Interfaces* **6**, 6672 (2014).
10. S. Ramdon, B. Bhushan and S. C. Nagpure, *J. Power Sources* **249**, 373 (2014).
11. Q. P. McAllister, K. E. Strawhecker, C. R. Becker and C. A. Lundgren, *J. Power Sources* **257**, 380 (2014).
12. C. Shen, S. Wang, Y. Jin and W. Q. Han, *ACS Appl. Mater. Interfaces* **7**, 25441 (2015).
13. L. Wang, D. Deng, L. C. Lev and S. Ng, *J. Power Sources* **265**, 140 (2014).
14. S.-K. Jeong, M. Inaba, T. Abe and Z. Ogumi, *J. Electrochem. Soc.* **148**, A989 (2001).
15. A. Cresce, S. M. Russell, D. R. Baker, K. J. Gaskell and K. Xu, *Nano Lett.* **14**, 1405 (2014).
16. W. Li, A. Xiao, B. L. Lucht, M. C. Smart and B. V. Ratnakumar, *J. Electrochem. Soc.* **155**, A648 (2008).